*J. Fluid Mech.* (1967). *vol.* 29, *part* 1, *pp.* 93–111
*Printed in Great Britain*



# Transition in oscillating boundary layer flows

By H. J. OBREMSKI
Research Department, Martin Company, Baltimore, Maryland
AND A. A. FEJER
Illinois Institute of Technology, Chicago, Illinois

(Received 24 March 1966)

An experimental investigation of transition phenomena in non-steady boundary layers of sinusoidally oscillating flows was conducted, and the effect of various parameters on the transition process was observed.

The manner in which transition occurs appears to be related to a dimensionless grouping designated as the non-steady Reynolds number, $(Re)_{NS} = L\Delta U/2\pi\nu$. When this number exceeds a certain critical value, transition begins with turbulent bursts appearing periodically at the frequency of the free stream oscillation; these are preceded by instability waves having the appearance of a Tollmien–Schlichting instability. The transition Reynolds number depends, in this case, only on the amplitude of the free stream oscillations and not on their frequency, at least to the first order. Below a critical value of this parameter, transition occurs at a relatively constant Reynolds number which appears independent of the amplitude and frequency of the oscillation, at least over the range tested.

When the bursts appear periodically, their development appears to occur in two succeeding phases: an initial or 'creative' phase marked by a sequential appearance of turbulence upstream and rapid development and a latter or 'convective' phase marked by turbulent spots having relatively constant leading and trailing edge velocities.

The dimensionless amplitude, $\Delta U/U_\infty$, of the imposed oscillations was varied from 0·014 to 0·29 while the oscillation frequencies extended from 4·5 to 62 c/s. Pressure gradients imposed on the flat plate model during the course of the study are given by $dC_p/dx = -0{\cdot}004$/ft., $-0{\cdot}081$/ft. and 0·045/ft. where $C_p = 2p/\rho U_\infty^2$ and $x$ is the distance (ft.) along the plate.

## 1. Introduction

All flows occurring in nature or as a result of man's engineering and scientific endeavours exhibit some degree of unsteadiness. The unsteadiness may be due to time-dependent boundary conditions or it may be the result of an instability arising from the small disturbances which are present in all flows. The onset of turbulence in the laminar boundary layer on a flat plate may be viewed as the final stage of such an instability. Although the effects of free stream turbulence, steady pressure gradients and roughness on boundary layer stability and transition have received considerable attention, little consideration has been given to the effect of large oscillations in the mainstream.

It was the object of this investigation to study experimentally the transition phenomena in a boundary layer when sinusoidal oscillations are imposed on the free stream. The oscillations considered were large in amplitude compared to the magnitude of the turbulent fluctuations in the free stream but were substantially lower in frequency.

The response of boundary layers to oscillations of low frequency has been treated by Moore (1951) and Lighthill (1954). Lin (1956), by assuming that the non-steady boundary-layer thickness was small compared to the steady thickness, was able to treat the response of the boundary layer to high-frequency oscillations. In these analyses, it was found that when the steady portion of the impressed pressure gradient was zero, the effect of the oscillation on the mean velocity profile was small. These analyses were extended and experimentally verified by Nickerson (1957) and Hill (1958).

When the question of the stability and transition of a non-steady boundary layer is broached, it should be realized that the criterion of stability in steady flow cannot be applied directly. In the steady state, a flow is considered stable to a small disturbance when it is monotonically damped with time. When the flow is unsteady, however, a disturbance may pass from stable to unstable regimes several times before its fate is ultimately determined. The instantaneous stability of flows has been considered by Shen (1960). Conrad & Criminale (1965*a*, *b*), by using a variational technique, have been able to determine sufficient conditions for the stability of several non-steady flows. Some experimental stability studies of a boundary layer on a flat plate with the mainstream undergoing small and slow oscillations have been conducted by Kobashi & Onzi (1962) with the aid of the vibrating ribbon technique.

To the authors' knowledge, the only extensive experimental study of the transition process in two-dimensional non-steady boundary layers on flat plates was that of Miller & Fejer (1964). They imposed sinusoidal oscillations on the flow over a flat plate and investigated their effect on the transition phenomena occurring in the boundary layer. During this investigation, it was found that the transition Reynolds number† was dependent on the amplitude parameter, $N_A = \Delta U/U_\infty$, and independent of the oscillation frequency, $\omega$, over the range of frequencies considered (4·5–125 c/s). In the transition region, the appearance of the turbulent bursts was periodic in contrast to the randomness that is characteristic of transition in steady flows, while the transition length was observed to depend on the frequency parameter, $\omega\nu/U_\infty^2$. The present study was conducted in the same facility and may be considered an extension of this earlier work.

## 2. Experimental apparatus

The investigation was conducted at Illinois Institute of Technology in a closed circuit $2 \times 2$ ft. wind-tunnel having, under steady-flow conditions, a velocity

† The transition Reynolds number, $(Re)_{tr} = x_{tr}U_\infty/\nu$, is based on the mean velocity of the free stream, $U_\infty$, and the minimum distance from the leading edge, $x_{tr}$, at which turbulence first appears in the boundary layer, i.e. the intermittency, $\gamma$, becomes greater than zero. Correspondingly, the turbulent Reynolds number, $(Re)_{tu}$, is based on the distance, $x_{tu}$, at which the boundary layer becomes turbulent, i.e. $\gamma$ becomes equal to unity.

range from 10 to 145 ft./s and a turbulence level of approximately 0·15–0·20 %. When operated in the non-steady mode, the maximum tunnel velocity was reduced to about 115 ft./s while the free stream turbulent intensity increased to approximately 0·2 %.

Oscillations of the free stream produced by means of a variable speed-rotating shutter valve, located at the end of the test section, covered a frequency range from 4·5 to 62 c/s. Variations in amplitude were achieved by using shutter blades of different widths; the widest blades produced the largest amplitudes but also reduced the maximum attainable flow velocities. The amplitude was also dependent on shutter speed.

In order to minimize any possible effects of the wave shape on the phenomena under study, the investigations were limited to flow conditions resulting in the most sinusoid-like oscillations. This occurred at oscillation frequencies near the longitudinal frequency of the tunnel (10·4 c/s) and its harmonics with the maximum amplitude being, however, considerably reduced at the higher harmonics.

The wind tunnel, test set-up and hot-wire equipment used in this study are basically the same as described by Miller & Fejer (1964); however, certain relevant modifications were made.

The shape of the leading edge of the flat plate was changed, and the adjustable flap which was located above the trailing edge of the plate on the ceiling of the test section was eliminated. The latter served to position the stagnation point on the upper surface of the leading edge which consisted of a 10° wedge, sharpened from below. These changes were made when turbulent bursts observed downstream of the leading edge were traced to the movement of the stagnation point around the leading edge during large amplitude oscillations. The new leading edge, $\frac{1}{4}$ in. thick at its base and 6 in. long, was formed by two intersecting circular arcs of large radius, tangent to the upper and lower surfaces of the plate, with the distance between the leading edge and the point of tangency being 4 and $2\frac{5}{16}$ in., respectively. The resulting leading edge shape was similar to that used by Schubauer & Skramstad (1943). Another change, consisting of the elimination of static pressure taps located along the centreline of the plate, was made when the coupling between the oscillating pressure field in the tunnel and the air contained in the tubing attached to the pressure taps was discovered to produce disturbances triggering transition. The usable length of the new plate was 62·5 in. Finally, the hemispherical epoxy nose of the boundary-layer probe, which in the earlier study was straight and positioned normal to the surface, was replaced by a wedge-shaped tip which was inclined forward, included a 20° angle with the upper surface of the plate and extended several inches upstream from its $\frac{1}{4}$ in. diameter vertical stem.

With the plate in a horizontal position, the streamwise pressure gradient was approximately zero ($dC_p/dx = -0{\cdot}004$/ft.) over the entire plate except the leading edge section. When a favourable pressure gradient was required, the plate was inclined relative to the direction of the free stream at an angle of $-2°$. This produced a reasonably constant pressure gradient of $dC_p/dx = -0{\cdot}081$/ft. In this configuration, a flap was used in front of and below the leading edge of the inclined plate to reduce the distance required by the pressure gradient to attain its

constant value. To produce a non-favourable pressure gradient, $dC_p/dx = 0{\cdot}045/$ ft., a long airfoil-shaped contour made of styrofoam was attached to the ceiling of the test section, and a styrofoam bump placed on the floor of the test section just below the leading edge of the plate served to maintain the stagnation point on the upper side of the plate. A photograph of this configuration is shown in figure 1, plate 1. The streamwise pressure distribution was determined with a static pressure probe positioned at a distance of $\frac{3}{8}$ in. above the plate.

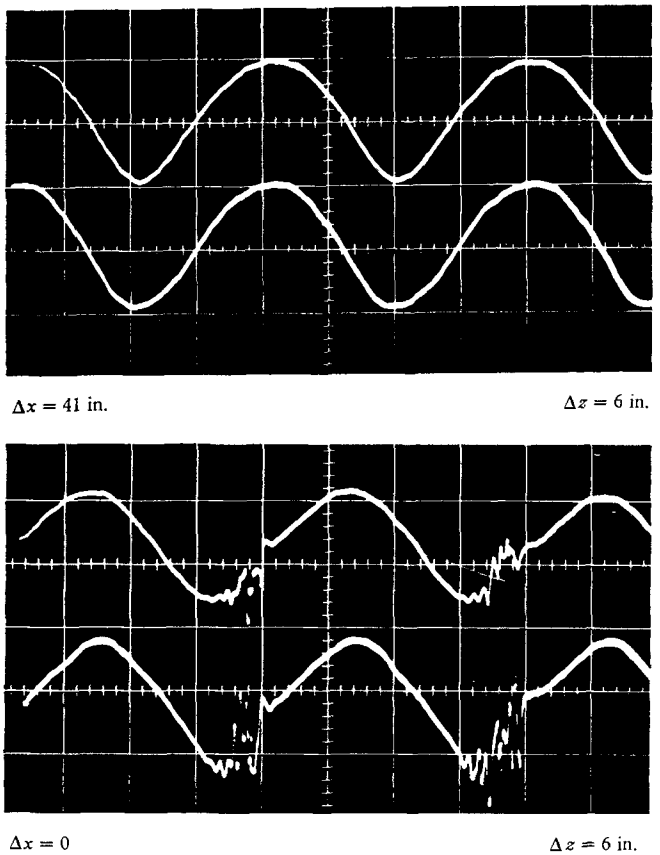


Figure 2. Velocity traces illustrating the transverse and lateral independence of the velocity oscillation. $U_\infty = 50$ f/s, $N_A = 0{\cdot}15$, $\omega = 12{\cdot}5$ c/s, sweep 20 ms/cm.

## 3. Preliminary measurements

The nature of the velocity oscillations employed in this study is characterized by the photographs of figure 2. The first photograph shows the mainstream oscillation sensed by two probes, one of which (lower trace) was located on the centreline and 41 in. downstream of the other which was 18 in. behind the leading edge. The spanwise distance between the two probes was 6 in. The two waveforms are virtually identical indicating that the oscillations were essentially independent of their streamwise position. The very slight phase lead exhibited by the downstream probe, which was approximately 15 in. from the shutter valve, is indicative of the incompressible character of the flow.

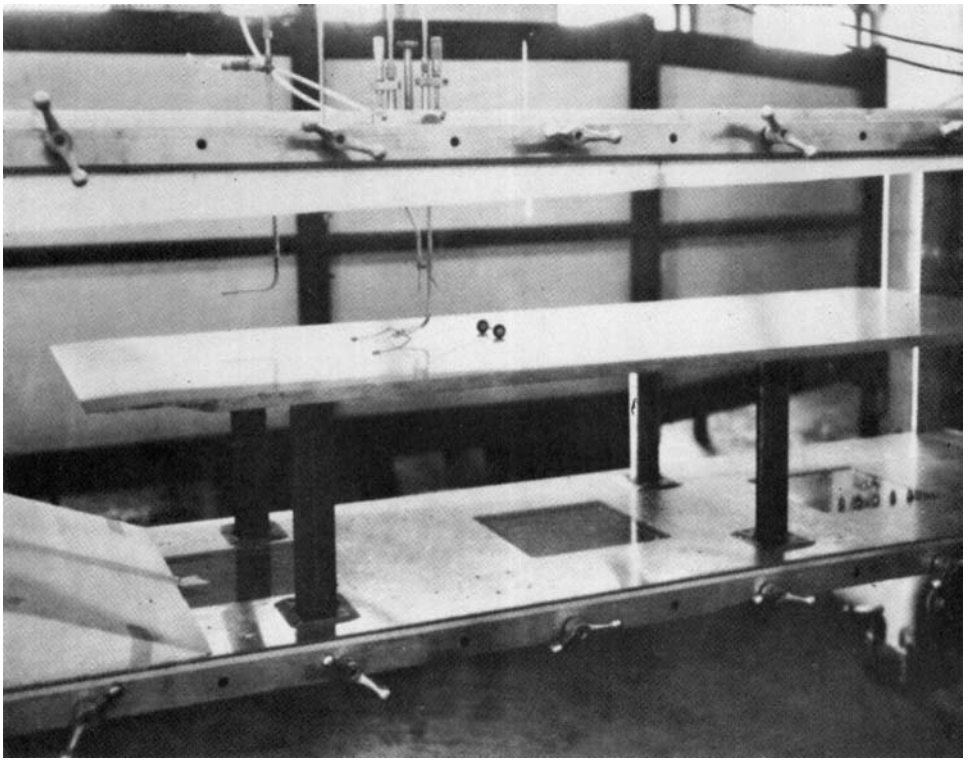

FIGURE 1. Test section with the adverse pressure contours in place.

The conditions shown were typical of those used in the major portion of the experiment. At higher frequencies, e.g. 60 c/s, the amplitude did vary somewhat with $x$; however, little data were taken at these conditions.

The second photograph was obtained with the probes located in the transition region of the boundary layer at the same streamwise position but with a spanwise separation of 6 in. The boundary-layer thickness at this point was approximately 0·15 in. Locations of the leading and trailing edges of the turbulent burst are identical, although the fine details of the burst and the waves which precede it are not.† These photographs indicate that the oscillation imposed on the mainstream was predominantly two-dimensional, essentially independent of $x$ and of sufficient strength to correlate, in the spanwise direction, the beginning and end of the turbulent burst in the boundary layer undergoing transition.

| $\frac{dC_p}{dx}$(1/ft.) | $T$ (%) | $(Re)_{tr} \times 10^{-6}$ (dimensionless) | $(Re)_{tu} \times 10^{-6}$ (dimensionless) |
|---|---|---|---|
| −0·004 | 0·15 | 2·05 | 3·5 |
| 0·045 | 0·20 | 0·92 | 1·1 |
| −0·081 | 0·15 | 3·40 | — |

TABLE 1. Turbulent intensity, transition and turbulent Reynolds numbers in steady flow

The tunnel and instrumentation were checked out by measuring the transition and turbulent Reynolds numbers in steady flow over a flat plate with zero and adverse pressure gradients. (Because of the limitations in plate length and flow velocity, fully turbulent flow was not attainable with a favourable pressure gradient.) Table 1 shows the results of these measurements including the attendant free stream turbulent intensities [$T = (\overline{u^2}/U_\infty)^{\frac{1}{2}} \times 100$]. It is seen that in the 'zero' pressure gradient case ($dC_p/dx = -0{\cdot}004$/ft.), the transition and turbulent Reynolds numbers are in fair agreement with the results interpolated from the data of Schubauer & Skramstad (1943), i.e. $(Re)_{tr} = 2{\cdot}3 \times 10^6$ and $(Re)_{tu} = 3{\cdot}8 \times 10^6$ at $T = 0{\cdot}15\,\%$.

In addition to the measurements shown in table 1, laminar boundary-layer profiles were determined in steady flows, and mean velocity distributions were made for a particular oscillating flow condition. It was found, as reported earlier by Nickerson (1957) and Hill (1958), that the Blasius profile adequately represents the mean velocity in a non-steady flow with a zero pressure gradient. A shift in phase of the velocity oscillation in the boundary layer relative to the free stream predicted in the analyses of Lighthill (1954) and Lin (1956) and verified experimentally by Hill (1958) was also observed in the present investigation as shown in figure 3 where the present data are compared with Hill's experimental

† The term 'turbulent burst' as it is used in this paper refers to the duration in time of the turbulence at a fixed value of $x$. This interval is directly measurable from the oscilloscope trace. The term 'turbulent spot' will refer to the spatial extent of a patch of contiguous turbulence, the downstream edge of the spot being called its leading edge. As we have seen, the turbulent spot appears to extend ribbonlike across the plate and in this it differs from the three-dimensional spot of steady boundary-layer transition.

results obtained under somewhat similar flow conditions. The agreement between these curves is fair considering the differences in experimental apparatus and instrumentation. This phase shift was not detected in the earlier investigation of Miller & Fejer (1964). It is believed that in their study this phenomenon was masked by streamline distortions due to the tip of their probe which was normal to the surface rather than pointing into the flow.

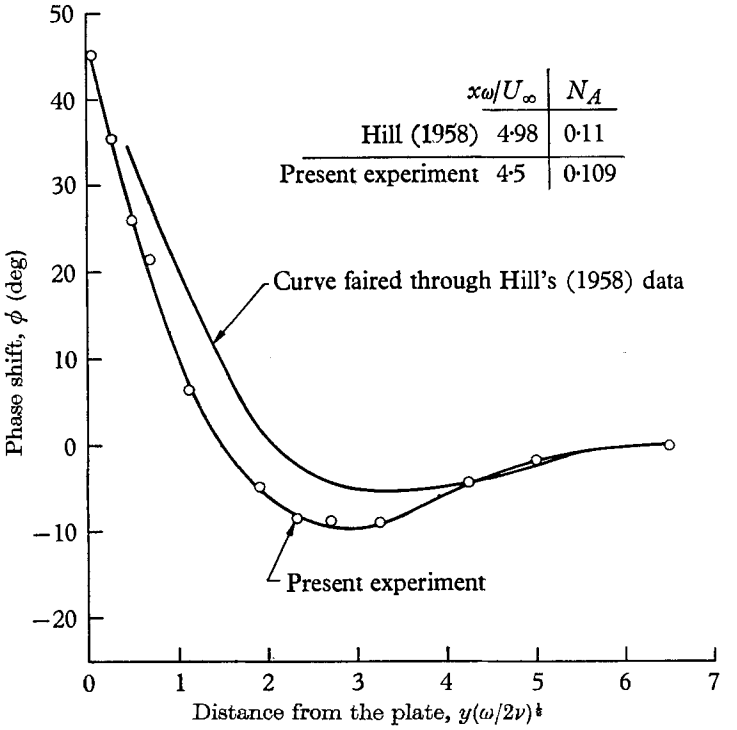


FIGURE 3. Velocity phase shift through an oscillating laminar boundary layer.

## 4. Transition in oscillating boundary-layer flows

The transition Reynolds number, $(Re)_{\mathrm{tr}}$, has been measured for the series of flow conditions summarized in table 2. It will be shown that the transition Reynolds numbers appear to lie along one of two curves depending upon whether a dimensionless grouping, herein called the non-steady Reynolds number $(Re)_{NS} = L\Delta U/2\pi\nu$, exceeds or is less than certain critical values. The characteristic length $L$, is defined as the length travelled by a fluid particle in the mainstream during one cycle of the imposed oscillation, i.e. $L = U_\infty/\omega$, and the characteristic velocity, $\Delta U$, is the amplitude of the oscillation.

In the following, the details of the transition process are described as observed over various ranges of the non-steady Reynolds number.

### (*a*) *Zero pressure gradient;* $(Re)_{NS} > 27{,}000$

Within this regime, the amplitude parameter, $N_A = \Delta U/U_\infty$, was varied from 0·039 to 0·27, and the oscillation frequency ranged from 4·5 to 14·7 c/s. The

| Run | $U_\infty$ (ft./s) | $N_A$ | $\omega$ (c/s) | $(Re)_{NS} \times 10^{-4}$ | $(Re)_{tr} \times 10^{-5}$ | $(Re)_{tu} \times 10^{-6}$ |
|---|---|---|---|---|---|---|
| | | | Zero pressure gradient | | | |
| *1 | 64·8 | 0·250 | 12·1 | 7·5 | 2·94 | 2·03 |
| *2 | 68·0 | 0·270 | 11·2 | 9·6 | 2·75 | 2·03 |
| 3 | 58·5 | 0·137 | 4·5 | 8·7 | 5·49 | 3·43 |
| *4 | 62·5 | 0·216 | 12·6 | 5·9 | 2·90 | 2·43 |
| 5 | 105·2 | 0·064 | 10·4 | 5·8 | 8·60 | — |
| 6 | 85·0 | 0·063 | 16·0 | 2·4 | 17·50 | — |
| *7 | 85·0 | 0·103 | 12·6 | 5·0 | 5·80 | — |
| *8 | 88·2 | 0·150 | 10·6 | 9·4 | 4·73 | — |
| 9 | 64·0 | 0·145 | 14·7 | 3·5 | 4·57 | 2·51 |
| *10 | 63·8 | 0·175 | 10·0 | 6·0 | 3·92 | 2·05 |
| 11 | 115·4 | 0·039 | 13·9 | 3·2 | 11·4 | — |
| *12 | 117·0 | 0·050 | 11·5 | 5·1 | 9·38 | — |
| 13 | 52·5 | 0·155 | 13·0 | 2·8 | 4·0 | — |
| 14 | 54·5 | 0·150 | 12·8 | 2·9 | 4·0 | 1·45 |
| *15 | 54·5 | 0·150 | 12·8 | 2·9 | 3·39 | 1·45 |
| 16 | 71·5 | 0·080 | 12·6 | 2·73 | 7·56 | — |
| 17 | 78·0 | 0·089 | 12·6 | 3·63 | 6·87 | — |
| 18 | 84·5 | 0·102 | 12·6 | 4·92 | 5·61 | — |
| 19 | 116·8 | 0·014 | 20·0 | 0·85 | 14·6 | 3·35 |
| 20 | 116·5 | 0·019 | 32·3 | 0·70 | 14·9 | 3·32 |
| 21 | 114·5 | 0·022 | 34·4 | 0·78 | 15·9 | 3·18 |
| 22 | 114·1 | 0·017 | 49·0 | 0·38 | 15·6 | 3·12 |
| 23 | 83·2 | 0·042 | 17·0 | 1·50 | 15·4 | — |
| 24 | 83·0 | 0·043 | 23·9 | 1·04 | 15·0 | — |
| 25 | 77·5 | 0·030 | 62·0 | 0·24 | 16·4 | — |
| 26 | 78·5 | 0·037 | 52·0 | 0·12 | 16·0 | — |
| 27 | 81·5 | 0·044 | 22·5 | 1·10 | 15·1 | — |
| 28 | 59·0 | 0·085 | 36·0 | 0·68 | 16·0 | — |
| 29 | 58·5 | 0·092 | 24·1 | 1·13 | 16·0 | — |
| 30 | 66·0 | 0·074 | 12·6 | 2·16 | 16·6 | — |
| | | | Favourable pressure gradient | | | |
| S-1 | 46·5 | 0·268 | 11·1 | 4·55 | 3·60 | — |
| S-2 | 50·7 | 0·215 | 13·3 | 3·54 | 4·14 | 1·50 |
| S-3 | 53·8 | 0·243 | 12·2 | 4·63 | 3·69 | — |
| S-4 | 52·7 | 0·227 | 12·4 | 4·24 | 3·84 | — |
| S-5 | 57·0 | 0·280 | 11·3 | 6·61 | 3·35 | 1·75 |
| | | | Adverse pressure gradient | | | |
| D-1 | 59·5 | 0·212 | 11·0 | 6·02 | 3·20 | 1·44 |
| D-2 | 58·0 | 0·110 | 4·59 | 6·95 | 4·90 | 1·85 |
| D-3 | 61·5 | 0·091 | 23·3 | 1·26 | 5·53 | 0·92 |
| D-4 | 61·6 | 0·064 | 33·9 | 0·61 | 6·95 | 0·92 |
| D-5 | 77·5 | 0·085 | 12·4 | 3·48 | 5·94 | 2·11 |
| D-6 | 82·5 | 0·045 | 23·2 | 1·15 | 7·97 | 1·32 |
| D-7 | 82·0 | 0·047 | 4·55 | 6·03 | 7·92 | 14·7 |
| D-8 | 81·5 | 0·046 | 37·0 | 0·72 | 7·84 | 1·16 |

* See text page 106 for explanation.

TABLE 2. Summary of flow conditions and transition results

results of these tests, summarized in table 2 (runs 1–5, 7–18), show that the transition Reynolds number is a function of the amplitude parameter and does not depend on the oscillation frequency, at least to the first order. These findings shown graphically in figure 4, are in qualitative agreement with the results of Miller & Fejer (1964) represented by the faired curve. (Their definition of the amplitude parameter is, however, $N_A = 2\Delta U/U_\infty$.) The quantitative difference between the results of the two studies may be attributable to the differences in leading edge shape and the influence of the static pressure taps that have been already described.

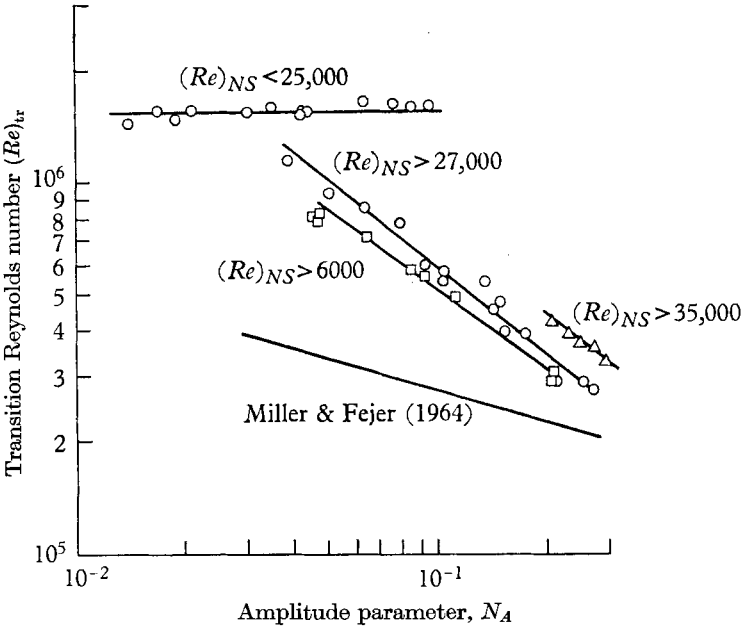


FIGURE 4. Transition Reynolds number as a function of the amplitude parameter for three pressure gradients. ○, $dC_p/dx = 0{\cdot}004$/ft.; △, $dC_p = -0{\cdot}081$/ft.; □, $dC_p/dx = 0{\cdot}045$/ft.

In figure 5, a series of photographs taken from run 15 shows the development of transition. The upper trace in each photograph represents the oscillating component of the mainstream velocity, and the lower trace records the velocity oscillations in the boundary layer where the local mean velocity was approximately $0{\cdot}5U_\infty$. The time co-ordinate for all traces increases to the right. It should be noted that successive photographs do not show the development of the same turbulent burst; however, since the flow is incompressible and the turbulent bursts will be seen to occur periodically, the upper trace assumes the role of a timing signal and it becomes possible to describe the growth of the turbulent burst in a Lagrangian sense based on Eulerian type measurements. One such measurement is illustrated in the fourth photograph of figure 5, where $\tau_i$ and $\tau_0$ represent the time lapse between the velocity minimum of the mainstream and the leading and trailing edges, respectively, of the succeeding turbulent burst.

The first photograph of figure 5, taken above the leading edge, represents the velocity oscillation in the free stream. In the second photograph, recorded at

$x = 10$ in., disturbance waves of essentially a single frequency are present in the trough of the boundary-layer trace. At the 14 in. position, these waves are increased in amplitude, and a turbulent burst appears on the interior of the wave packet midway up the positive slope of the imposed oscillation. Proceeding downstream to the 26 in. position, the turbulent burst has increased in duration and is still preceded in time by disturbance waves, however, no disturbance waves are evident at its trailing edge. By the time the turbulent burst has reached the 32 in. position, it is no longer preceded by the disturbances and it continues to spread into the laminar interval until, at $x = 60$ in., the boundary layer is fully turbulent.

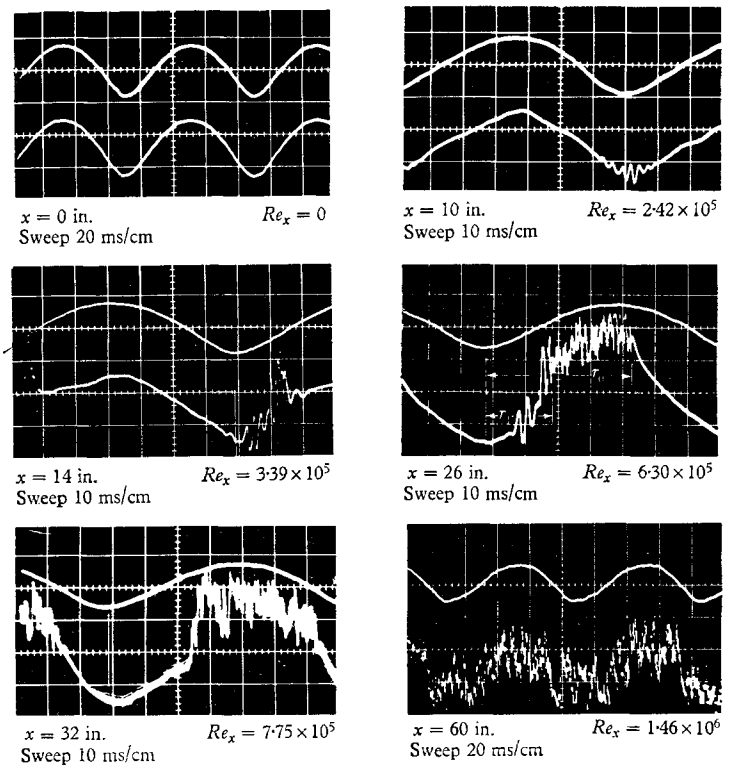


FIGURE 5. Oscilloscope traces illustrating the initiation and development of the turbulent burst in the transition region. Upper trace: free stream. Lower trace: boundary layer. Run 15, $U_\infty = 54{\cdot}5$ ft./s, $N_A = 0{\cdot}15$, $\omega = 12{\cdot}8$ c/s.

At the larger values of the non-steady Reynolds numbers in this range (say $(Re)_{NS} > 40{,}000$), the turbulence appeared regularly during each cycle of the imposed oscillation with the initial burst of turbulence appearing close to the trough of the waveform. This periodic behaviour has been noted previously by Miller & Fejer (1964) and is referred to as periodic transition. As the non-steady Reynolds number decreased toward 27,000, however, the periodicity of the initial burst became weaker (i.e. it did not always appear during each and every cycle of the imposed oscillation), and it occurred closer to the crest of the waveform as

seen in figure 5 ($x$ = 14 in.), where $(Re)_{NS}$ = 29,000. This slight initial aperiodicity disappeared as one proceeded farther downstream into the transition region.

The frequency of the small disturbances, such as seen in figure 5 in the trough of the boundary-layer trace recorded at $x$ = 10 in., can be determined with fair accuracy ($\pm$ 10 %) directly from the traces recorded at various positions upstream of the beginning of the transition region. Such data were obtained from many runs and when plotted in figure 6 against Reynolds number, based on the dis-

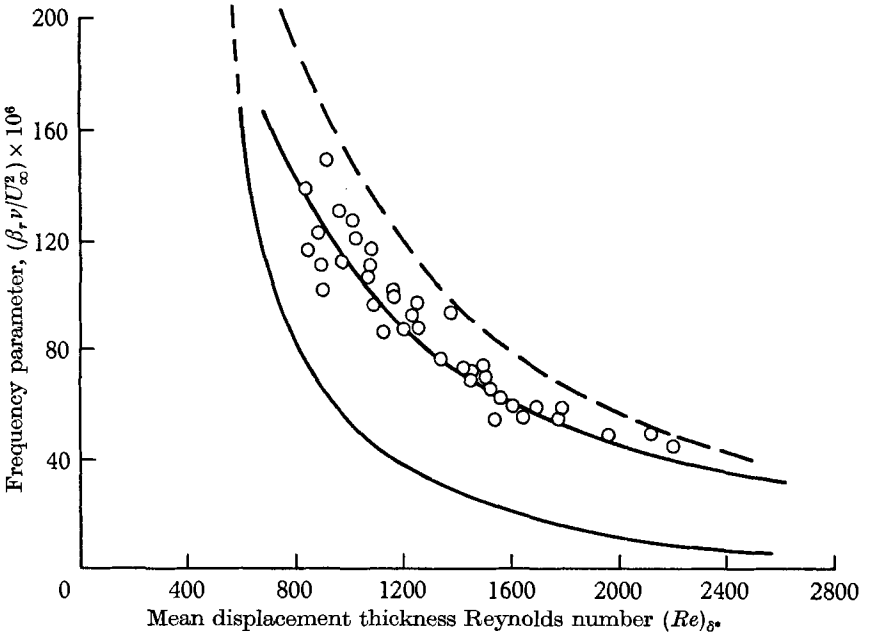


FIGURE 6. Non-dimensional frequency of the instability waves occurring in an oscillating boundary layer as a function of the mean displacement thickness Reynolds number. O, non-steady flow; ——, Tollmien (1929); – – –, Timman–Zaat (1956).

placement thickness of the mean flow, were found to lie in the vicinity of branch II of the Tollmien–Schlichting curve of neutral disturbances for a laminar boundary layer on a flat plate. Also shown for comparison is the Timman–Zaat curve of neutral oscillations. Considering the similar trends of the data and the theoretical curves of neutral stability as well as the growth and decay of disturbances at small $x$'s, it seems plausible that the disturbances may be amplified Tollmien–Schlichting waves.

For values of the frequency parameter, $x\omega/U_\infty$,† in the relatively narrow range between 0·6 and 1·3, the disturbance waves appeared first near the trough of the wave. It is recalled that this parameter is proportional to the square of the ratio between the viscous boundary-layer thickness and the so-called '$ac$' boundary-layer thickness and is sometimes used to distinguish between the low frequency or quasi-steady, the intermediate frequency and high-frequency regimes in oscillating boundary-layer flows. The values delineating the regimes are somewhat arbitrary and typical values might be: quasi-steady range $x\omega/U_\infty < 1$,

† $\omega$ here has dimensions rad/s.

intermediate frequency range $1 < x\omega/U_\infty < 10$ and high-frequency range $x\omega/U_\infty > 10$ (Farn & Arpaci 1966). Thus, the range of values at which the disturbance waves were first detected straddles the upper limits of the quasi-steady regime and the lower end of the intermediate frequency regime. The fact that the disturbance waves arose while the boundary layer might still be considered in the quasi-steady condition and had frequencies which were in close proximity to branch II of the Tollmien–Schlichting diagram for steady boundary layers might suggest that the stability of the flow could be analyzed under a quasi-steady assumption, i.e. treating the instantaneous velocity profile at each instant as a steady flow and determining if a superimposed disturbance will grow or decay at the instant considered.

It is also noteworthy that although the initial instability was first detected in the trough, at downstream positions the trough appears free of these disturbances. This might be due to a change in the stability characteristics at the larger values of $x\omega/U_\infty$ or due to a calming period following the passage of a turbulent spot. The results of this investigation cannot be used to evaluate the first of these possibilities; however, the second possibility will be explored later in the paper when data concerning the convective velocity of the turbulent spot are presented.

### (*b*) *Zero pressure gradient*; $(Re)_{NS} < 25{,}000$

In this regime, the amplitude parameter was varied from 0·014 to 0·092, and the oscillation frequency ranged from 12·6 to 62 c/s. The results of these tests are included in figure 4 and summarized in table 2 (runs 6 and 19–30).

It may be observed from the appropriate curve of figure 4 that the transition Reynolds number is relatively constant, approximately $1{\cdot}6 \times 10^6$, and appears independent of both the amplitude parameter and the oscillation frequency, at least for the ranges tested. This value of the transition Reynolds number is somewhat less than that appropriate to a steady boundary-layer flow having the same free stream turbulent intensity. Here, the free stream turbulent intensity was approximately 0·2 % which in steady flow would correspond to a transition Reynolds number of $2{\cdot}1 \times 10^6$ (Schubauer & Skramstad 1949). The turbulent bursts lacked the periodicity of the higher non-steady Reynolds number range ($(Re)_{NS} > 27{,}000$), although the upper portions of the wave-form closer to the crest were preferred for turbulent outbreak and development, as if tending to occur at the higher local Reynolds numbers. Because of this preference, the passage of turbulent bursts could not be characterized as occurring randomly in time, nor were they periodic in the sense of the $(Re)_{NS} > 27{,}000$ range; one could best describe them as 'aperiodic'.

The aperiodicity of the bursts together with the independence of transition Reynolds number on amplitude and frequency may suggest that the responsibility of the oscillation in promoting transition has changed from a 'dominant' role in the regime where the transition Reynolds number depends on the amplitude parameter and the transition is periodic to a 'co-operative' one in which it merely increases the local Reynolds number to values at which transition tends to be initiated. The concept of 'shifting co-responsibility' between flow characteristics promoting transition is not new and has been suggested by Morkovin (1958) as a

means of understanding other anomalous experimental results in transition. The present results are not sufficient to determine those flow characteristics to which the oscillation appears to have lost dominance as far as promoting transition is concerned, if indeed this is really the case.

(*c*) *Favourable pressure gradient*; $(Re)_{NS} > 35{,}000$

For this group of tests, the steady favourable pressure gradient was $dC_p/dx = -0{\cdot}081$/ft. Due to the stabilizing effect of the favourable pressure gradient, transition occurred only at the higher values of the amplitude parameter, $N_A = 0{\cdot}21$ to $0{\cdot}29$, which could be achieved only over a narrow range of frequencies near 12 c/s. The results of this group of tests are also incorporated in figure 4 and are listed in table 2 (runs S-1 to S-5). Transition was observed to be always periodic, with the transition Reynolds number again depending only on amplitude.

(*d*) *Adverse pressure gradient*; $(Re)_{NS} > 6000$

The steady adverse pressure gradient was $dC_p/dx = 0{\cdot}045$/ft., the amplitude parameter was varied from $0{\cdot}04$ to $0{\cdot}21$, and the oscillation frequency covered the range from $4{\cdot}5$ to 37 c/s. Under these conditions transition was periodic, the transition Reynolds number was again dependent on the amplitude parameter and independent of oscillation frequency. The results are listed under runs D-1 to D-8 in table 2 and appear also in figure 4. As the figure shows, the adverse pressure gradient had a destabilizing effect on the oscillating boundary layer.

## 5. Periodic transition, zero pressure gradient

It was mentioned above that under flow conditions where the transition is periodic it is possible to plot the space-time co-ordinates of the leading and trailing edges of the burst as they proceed downstream by using the mainstream trace as a timing signal. The curve presented in figure 7 represents such a plot of data taken from run 15; a portion of which was displayed in figure 5. In this run $U_\infty = 54{\cdot}5$ ft./s, $N_A = 0{\cdot}150$, and $\omega = 12{\cdot}8$ c/s. In figure 7, the abscissa, $x$, is the position along the plate while the ordinate, $\tau^*$, is the ratio of $\tau$, the time lapse between an event and the minimum of the mainstream velocity trace which preceded it in time, and $\bar{\tau}$ the period of the oscillation. Hence, in figure 7, points on a horizontal line indicate conditions along the plate at a given instant, while points in a vertical line depict changes with time at a fixed position. In particular, $\Delta\tau^*|_x$ denotes the intermittency or when multiplied by $\bar{\tau}$, the burst duration, while $\Delta x|\tau^*$ represents the streamwise dimension of a turbulent disturbance at a given instant. A positive slope indicates that the edge of the turbulent disturbance is moving downstream relative to the plate, a negative slope indicates the spreading of the edge of the turbulent disturbance in the upstream direction and the magnitude of the slope is inversely proportional to the velocity of the edge. In addition to the time-space co-ordinates of the laminar-turbulent boundary, the approximate extent of the instability wave packet contiguous to the turbulent spot at the beginning of its development is also shown.

From the curve of figure 7, it can be seen that a small turbulent spot appears at $\tau^* = 0{\cdot}1$ in the vicinity of a point located approximately 16 in. downstream of the leading edge. Initially, this spot spreads rapidly both in the upstream† and downstream direction and ultimately attains at $\tau^* = 0{\cdot}8$, a length of approximately 27·5 in. At that time, its leading edge merges with the trailing edge of the preceding spot and it enters the fully turbulent region of flow. It appears that in this

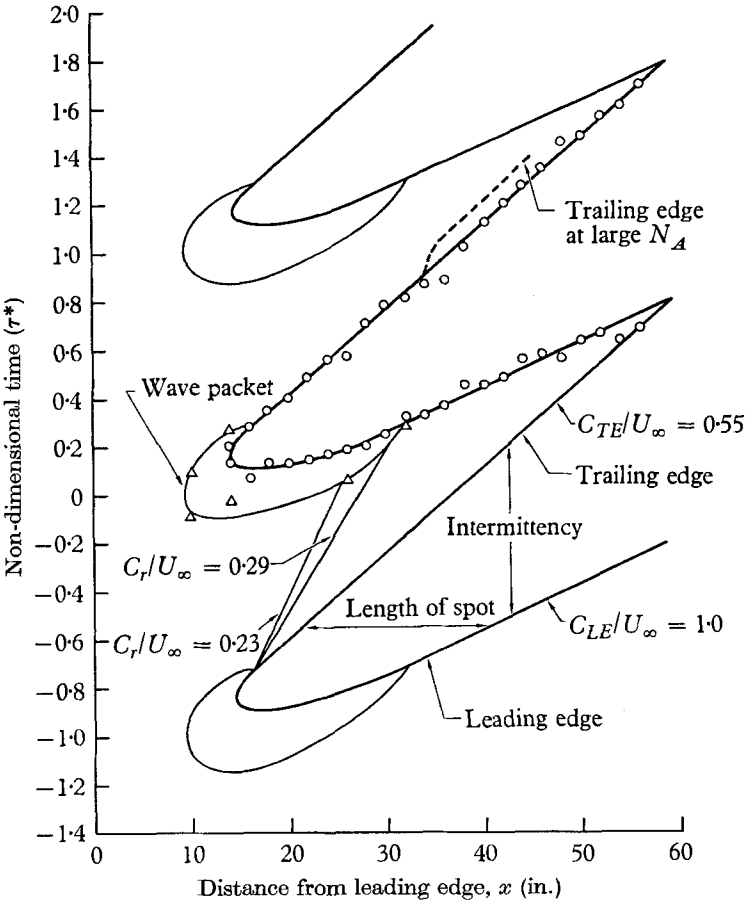


FIGURE 7. Time–space distribution of the turbulent spot during transition, run 15, $U_\infty = 54{\cdot}5$ ft./s, $N_A = 0{\cdot}15$, $\omega = 12{\cdot}8$ c/s.

case one can distinguish three distinct regions of flow: a region of instability located upstream of $x = 14$ in.; a fully turbulent region downstream of 58·5 in.; and an intermediate region containing, in addition to instability waves, periodically occurring laminar and turbulent spots. This region is identifiable with the transition region of steady boundary layers where, however, the spots are of course neither two-dimensional nor periodic.

† The description 'spreading upstream' implies observed sequential appearance of the turbulent edge at decreasing values of $x$, at least initially. At this stage of our knowledge, to imply a mechanism for this upstream spreading would be premature.

In the transition region, the leading edge of the turbulent spot is preceded by instability waves in time and space up to $\tau^* = 0{\cdot}3$ and $x = 32$ in., while at the trailing edge the waves disappear at $\tau^* = 0{\cdot}3$ and $x = 16$ in. (Refer also to the appropriate photographs of figure 5.) The simultaneous emergence of the leading and trailing edges of the spot from the wave-packet at $\tau^* = 0{\cdot}3$ is probably a coincidence.

After the turbulent spot emerges from its sheath of instability waves, the velocities of its leading and trailing edges remain relatively constant throughout the remainder of the transition regime (an exception to this is noted below). In this latter portion of the transition region, the leading edge velocity, $C_{LE}$, for this run was equal to the mean velocity of the free stream while the velocity of the trailing edge, $C_{TE}$, was equal to $0{\cdot}55U_\infty$. Data for this run were taken in the boundary layer where the local mean velocity was $0{\cdot}5U_\infty$. Other data taken at essentially the same free stream conditions but with the probe positioned at $0{\cdot}7U_\infty$ and $0{\cdot}9U_\infty$ indicated that the velocity of the trailing edge was $0{\cdot}57U_\infty$ and $0{\cdot}64U_\infty$, respectively, while the velocity of the leading edge was unchanged, i.e. it was equal to $U_\infty$. The observed independence of $C_{TE}$ and $C_{LE}$ on time for this run is actually a reflexion of the relatively small amplitude ($N_A = 0{\cdot}15$). At larger amplitudes, the trailing edge of the burst experienced a decrease in velocity as it approached the trough of the oscillation, i.e. $\tau_0^* \doteq 0{\cdot}9$. Once through the minimum, i.e. $\tau_0^* \doteq 1{\cdot}1$, it resumed its previously constant value. This behaviour is illustrated in figure 7 by the dotted lines on the upper branch of one of the curves. In eight of the runs (marked by asterisks in table 2) the leading and trailing edge velocities of the turbulent spot were relatively constant for a considerable portion of the transition regime. The average leading edge velocity for the eight runs was $0{\cdot}88U_\infty$ with a standard deviation of $0{\cdot}12U_\infty$ while the average trailing edge velocity for these runs was $0{\cdot}58U_\infty$ with a standard deviation of $0{\cdot}06U_\infty$. Comparative values for a three-dimensional spot in steady flow reported by Schubauer & Klebanoff (1955) are $0{\cdot}88U_\infty$ and $0{\cdot}51U_\infty$, respectively.

Referring again to the curves of figure 7, contrast the relatively constant, downstream velocity of the turbulent spot in the absence of observable instability waves at its edges to its behaviour when surrounded by them. In their presence, the turbulence appears to spread initially both upstream and downstream, its leading edge moving downstream at velocities in excess of that of the mainstream. Subsequently, the velocity of the trailing edge of the turbulent spot changes from negative to positive and then approaches the constant value of $0{\cdot}55U_\infty$ as it emerges from the wave packet.† There appears to be sufficient contrast between the development of the turbulence when instability waves are present and its development in their absence to justify denoting these two modes of development by different names. The early mode of its development, when the turbulence is spreading through the observable large-amplitude instability waves will be referred to as the 'creative mode'. The apparent upstream spread of the trailing edge and the initially high leading edge velocity correspond to a growth rate of the turbulent spot substantially larger than those observed in steady

† Actually, in other periodic transition runs the extent of the apparent upstream spread of the turbulence was considerably greater than that shown in figure 7.

boundary layers. Farther downstream in the transition regime where the leading and trailing edges of the growing spot move at constant, but different rates, the term 'convective mode' will be used.†

In short the distinction between the two modes is primarily the magnitude of the growth rate, which appears to be associated with the presence or absence of observed large amplitude instability waves in proximity to the turbulent front. The creative and convective modes were observed in varying degrees for all runs in which the transition was periodic. During the transition examined in figures 5 and 7, the convective mode predominated. Below we shall examine some transition situations in an adverse pressure gradient case where the creative mode was found to dominate.

Let us consider first to what degree the calming effect may be responsible for the absence of instability waves in the trough of the trace as one proceeds downstream into the transition region, referring again to figure 7 and specifically to the front of the instability wave packet which recedes from $\tau^* = -0{\cdot}1$ at $x = 10$ in. to $\tau^* = 0{\cdot}29$ at $x = 32$ in. In order to determine whether the calming effect of the preceding spot may be at least in part responsible for the recession and eventual disappearance of the instability waves in the latter region of the transition zone, consider the appropriate results of Schubauer & Klebanoff (1955). They found that the passage of a turbulent spot 'swept clean' any instability waves from the fluid through which the spot passed. This calm period lasted until another turbulent spot or other instability waves arrived from upstream. This quiescent period was the result of the differences between the trailing edge velocity of the turbulent spot ($0{\cdot}51U_\infty$) and the propagation velocity of the disturbance waves following it. One of their experiments yielded $0{\cdot}23U_\infty$ as the velocity of the instability wave in the calm region, while a second experiment yielded $0{\cdot}29U_\infty$; both values being somewhat less than that of the two-dimensional wave calculated in stability theory. Since the instability waves detected in the present study seem to bear some resemblance to a quasi-steady flow (as suggested by the proximity to branch II in the Tollmein–Schlichting diagram), these values will be assumed here in an attempt to assess the possibility of a calming effect being responsible for the recession of the wave front and eventual abolition of waves in the latter portions of the transition region.

In the $(x, \tau^*)$-plane of figure 7, the duration of a possible calming period can be determined for a given location from the vertical distance between the branch of the curve representing the measured trailing edge velocity of the turbulent spot, $C_{TE}$, and a line corresponding to the assumed velocity of the instability wave, $C_r$. Two such lines representing values of $C_r$ equal to $0{\cdot}23U_\infty$ and $0{\cdot}29U_\infty$ are shown in the figure starting from $x = 16$ in. If the wave had a velocity $C_r = 0{\cdot}23U_\infty$ and had started immediately after the trailing edge of the spot passed the 16 in. position, this line would represent the extent to which the calming effect of a spot could be effective. Thus if the flow upstream of this line and outside the wave-packet appears quiescent this must be due to other causes. If the wave velocity

† One notes that the growing three-dimensional turbulent spots of Schubauer & Klebanoff (1955) are also convected downstream and that the two edges grow at different but constant rates, similar to those observed here.

were $0{\cdot}29U_\infty$, then the figure shows that calming should occur in the neighbourhood of $x = 30$ in. and $\tau^* = 0{\cdot}2$ and that it should last 0·038 sec. The region downstream of the $0{\cdot}29U_\infty$ line is seen to be free of instability waves, and thus the possibility exists that this may be due to calming. It would appear from the above discussion that the calming effect may play a role in terminating the creative period of transition and, by doing so, increase the length required for transition to be accomplished.

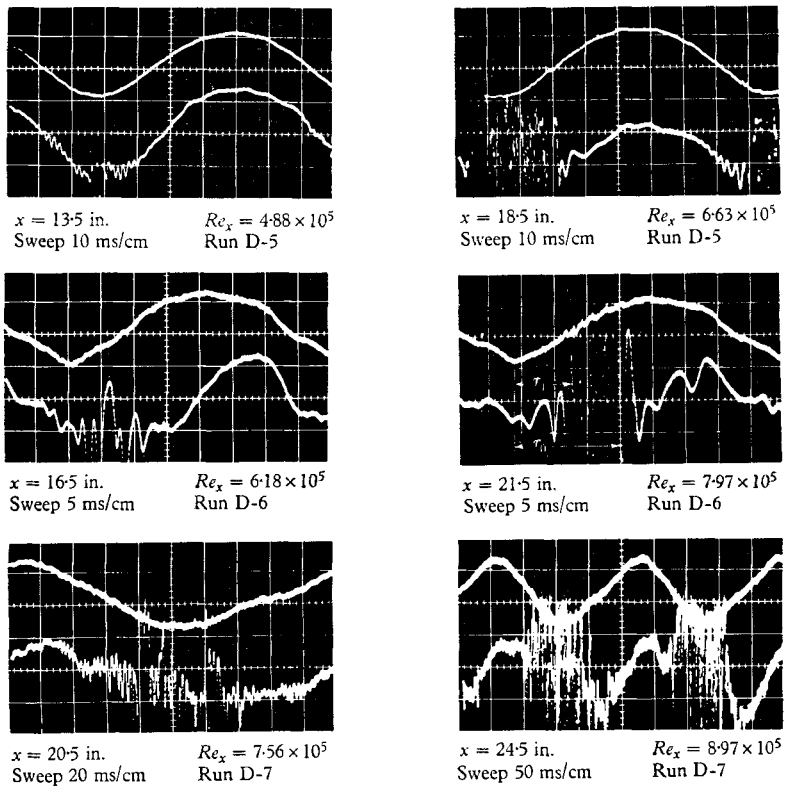


FIGURE 8. Oscilloscope traces illustrating the velocity fluctuations before and after the beginning of the transition region for three runs with a steady adverse pressure gradient. $dC_p/dx = 0{\cdot}045$/ft. Upper trace: free stream. Lower trace: boundary layer.

## 6. Periodic transition: adverse pressure gradient

An examination of transition diagrams constructed from data obtained during the imposition of a steady, adverse pressure gradient on the non-steady flow will serve to illustrate the topography of the transition region when the transition occurs primarily in the creative mode. This will be made apparent with the aid of figures 8 and 9 which refer to adverse pressure gradient ($dC_p/dx = 0{\cdot}045$/ft.) runs D-5, D-6 and D-7 made at approximately the same velocity of 80 ft./s. In figure 8 the top two photographs on the left were taken just upstream of the position where the first manifestation of turbulence was observed, while in the third photograph, the presence of 'spikes' may be indicative of turbulence in a very early

stage.† The photographs on the right side of figure 8 were taken just inside the transition region, and serve to illustrate the early development of the burst.

The co-ordinates of figure 9 are the same as those of figure 7. The curve of figure 9*a*, run D-5, is similar to that of figure 7 and establishes that under a steady adverse pressure gradient of the magnitude used here a considerable portion of the transition may occur in the convective mode.

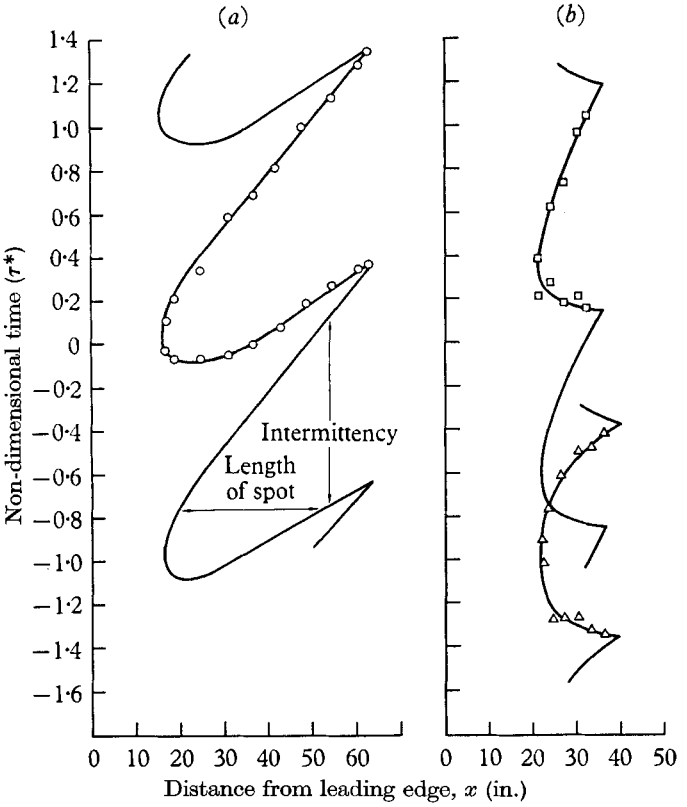


FIGURE 9. Time–space distributions of turbulent bursts during periodic transition under a steady adverse pressure gradient. $dC_p/dx$ = 0·045/ft. (*a*) Run D-5: ○, $N_A$ = 0·085, $\omega$ = 12·4 c/s; (*b*) Run D-6: □, $N_A$ = 0·043, $\omega$ = 23·2 c/s. Run D-7: △, $N_A$ = 0·047; $\omega$ = 4·55 c/s.

For the two runs D-6 and D-7 shown in figure 9*b* laminar flow does not, at any time, appear downstream of the turbulent flow region. Thus, in run D-6 it is as though a boundary line between laminar and turbulent regions advances and retreats with the period of the free stream oscillation over a section of surface located between $x$ = 21 in. and $x$ = 37 in.; in run D-7, the movements of the line cover the region between $x$ = 22 in. and $x$ = 40 in. Thus, the apparent upstream excursion of the turbulence in run D-6 was 16 in. while in run D-7 it was 18 in.

† This photograph illustrates the difficulty of determining precisely where the first turbulent burst appears. Under many of the flow conditions tested, however, the uncertainty connected with determining the beginning of the transition region was resolvable within an inch along the plate. The outbreak of turbulence was taken as the appearance of a burst of high frequency and amplitude compared with the waves surrounding it.

The upstream excursions cited here were the largest encountered during the study.

According to our definition, the transition in the runs D-6 and D-7 occur predominantly in the high rate creative mode. The very rapid growth rate of the creative mode in these two runs precluded the existence of the laminar tongues which appear in figure 9*a*.

When creative transition predominated, the wave-form was observed to be contaminated extensively with instability waves prior to the initial turbulent outbreak. A comparison between the photos of runs D-6 and D-7 and those of run D-5 serves to illustrate this point. Transition lengths in which the creative mode dominated were usually considerably shorter than in the case of convective transition where the calming effect may be partially responsible for prolonging the transition length.

## 7. Concluding remarks

The transition Reynolds number, as it has been used in this paper, is based upon the position where the intermittency becomes greater than zero, i.e. the vertical tangent to the curves of figure 9 or the minimum in $x$. The Reynolds number which corresponds to the horizontal tangent to the curves or the minimum in time over a cycle may also be significant since it corresponds to the birthplace of the spot during each cycle of the oscillation. The difference between these two represents the extent of the sequential appearance of turbulence upstream. To describe this process, unknown in steady flows, by the word 'propagate' would imply a mechanism of upstream triggering by downstream turbulence which at the present stage of our knowledge would be prejudging the matter.

The authors wish to acknowledge the financial support of this study under National Science Foundation Grant GP 2484. In addition, appreciation is expressed to Dr M. V. Morkovin of the Martin Company for stimulating discussions during the writing of the paper.

REFERENCES

Conrad, P. W. & Criminale, W. O. 1965*a* The stability of time dependent laminar flow: parallel flows. *J. Appl. Math. Phy.* **16**, 283.

Conrad, P. W. & Criminale, W. O. 1965*b* The stability of time dependent laminar flow: flow with curved streamlines. *J. Appl. Math. Phy.* **16**, 569.

Farn, C. L. & Arpaci, V. S. 1966 On the numerical solution of unsteady laminar boundary layers. *AIAA*, **4**, no. 4.

Hill, P. G. 1958 *Laminar boundary Layers in Oscillatory Flow.* Sc.D. Thesis, Massachusetts Institute of Technology.

Kobashi, Y. & Onzi, A. 1962 Stability of a boundary layer with a time dependent outside flow. *National Aero Lab., Tokyo, Japan.*

Lighthill, M. J. 1954 Response of laminar friction and heat transfer to fluctuations in stream velocity. *Proc. Roy. Soc.* A **224**.

Lin, C. C. 1956 Motion in the boundary layer with a rapidly oscillating external flow. *Proc. 9th Int. Congr. Appl. Mech.* IV.

Lin, C. C. 1957 *On the Instability of Laminar Flow and Its Transition to Turbulence.* Boundary Layer Research Symposium. Freeburg, Berlin: Springer.

MILLER, J. A. & FEJER, A. A. 1964 Transition phenomena in oscillating boundary layer flows. *J. Fluid Mech.* **18**, 438.

MOORE, F. K. 1951 Unsteady boundary-layer flow. *NACA Tech. Note*, no. 2471.

MORKOVIN, M. V. 1958 Transition from laminar to turbulent shear flow—a review of some recent advances in its understanding. *Trans. ASME*, pp. 1121–1128.

NICKERSON, R. J. 1957 The effect of free stream oscillations on the laminar boundary layer on a flat plate. Sc.D. Thesis, Massachusetts Institute of Technology.

SCHUBAUER, G. F. & SKRAMSTAD, H. K. 1948 Laminar boundary-layer oscillations and transition on a flat plate. *NACA Rept.* no. 909.

SCHUBAUER, G. F. & KLEBANOFF, P. S. 1955 Contributions on the mechanics of boundary-layer transition. *NACA Tech. Note*, no. 3489.

SHEN, S. F. 1960 Some considerations of the laminar stability of incompressible time-dependent base flows. *Nav. Ord. Rept* no. 6654.

TIMMAN, R., ZAAT, J. A. & BURGERHOUT, T. J. 1956 Stability diagrams for laminar boundary-layer flow. *National Aero Research Inst., Amsterdam, NLL Tech. Note*, no. F193.

TOLLMIEN, W. 1929 Uber die Entstehung der Turbulenz. English translation in *NACA Tech Memo*, no. 609, 1931.